Supplement of Atmos. Meas. Tech., 11, 5087–5104, 2018
https://doi.org/10.5194/amt-11-5087-2018-supplement

Atmospheric Measurement Techniques
Open Access
EGU

Supplement of

Real-time measurements of gas-phase organic acids using SF_6^- chemical ionization mass spectrometry

Theodora Nah et al.

Correspondence to: L. Gregory Huey (greg.huey@eas.gatech.edu)

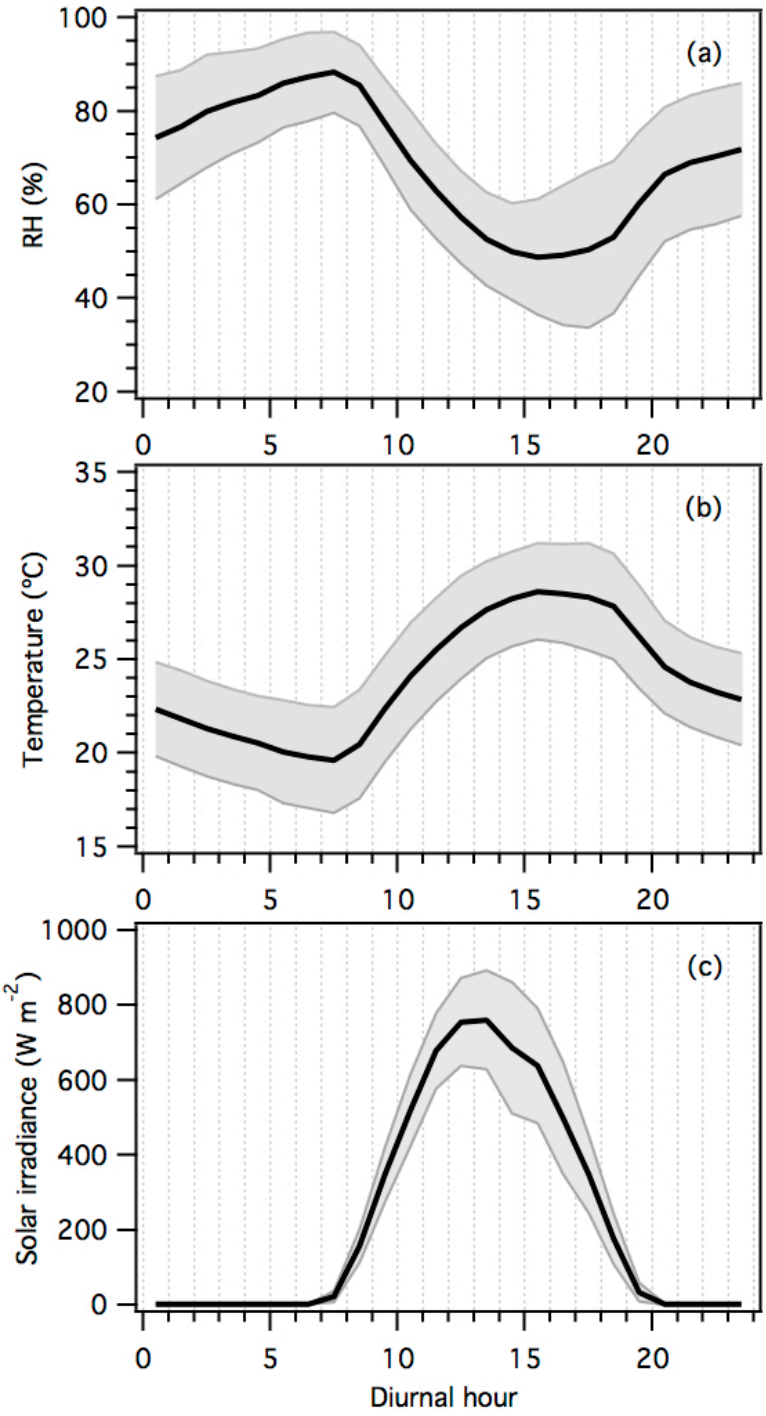

Figure S1: Diurnal trends of (a) relative humidity, (b) temperature, and (c) solar radiance. The lines within the shaded area represents the average values. The upper and lower boundaries of the shaded areas mark one standard deviation.

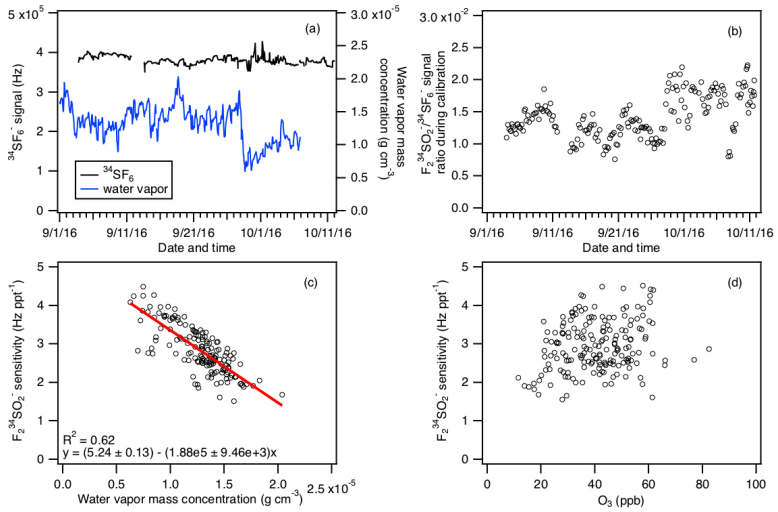

Figure S2: (a) Time series of $^{34}SF_6^-$ reagent ion signal and ambient water vapor concentration for the entire field study. The ambient water vapor mass concentrations are determined from ambient relative humidities and temperatures. (b) Time series of $F_2{}^{34}SO_2^-$ /$^{34}SF_6^-$ ion signal ratio obtained during calibration measurements. Panels (c) and (d) show the $F_2{}^{34}SO_2^-$ ion sensitivity obtained from calibration measurements as a function of ambient water vapor and O_3 concentrations. Data in panels (a) to (d) are displayed as 1-hour averages.

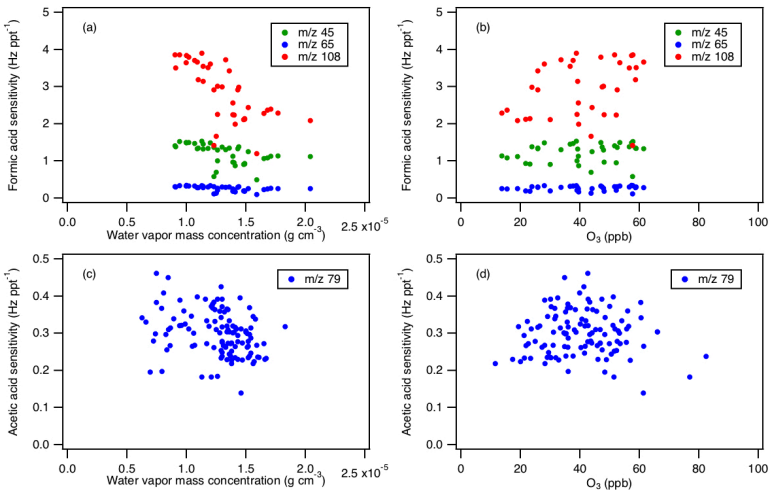

Figure S3: Panels (a) and (b) show the sensitivities of formic acid ions ($HCOO^-$ at m/z 45, $HCOO^-$•HF at m/z 65, and SF_4^- at m/z 108) obtained from calibration measurements as a function of ambient water vapor and O_3 concentrations. Panels (c) and (d) show the acetic acid sensitivity (CH_3COO^-•HF at m/z 79) obtained from calibration measurements as a function of ambient water vapor and O_3 concentrations.

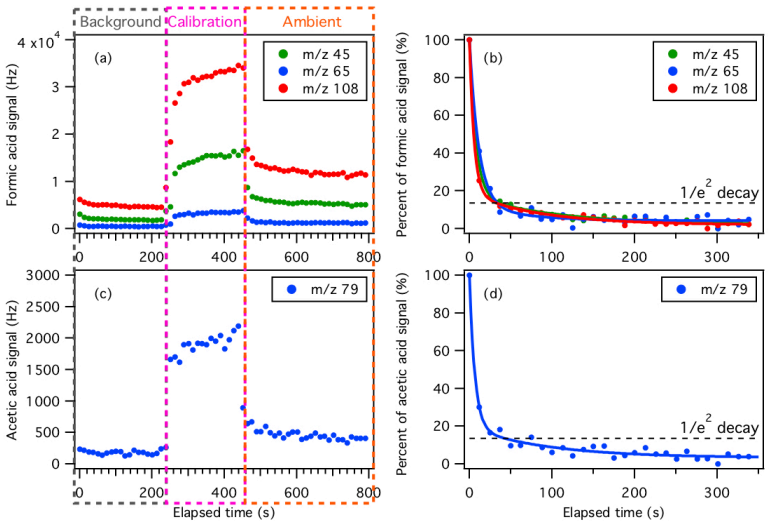

Figure S4: Example of the CIMS instrument response during switches between background, calibration and ambient measurements of (a) formic, and (c) acetic acids. Panels (b) and (d) show the percent of formic and acetic acid ion signals after the removal of a 6.75 ppb of formic acid and 5.87 ppb of acetic acid standard addition calibration as a function of time. The data shown here is 13 s time resolution data. Double exponential fits to each m/z ion are shown as colored solid lines. Black dashed lines show the times for the ions to decay to $1/e^2$.

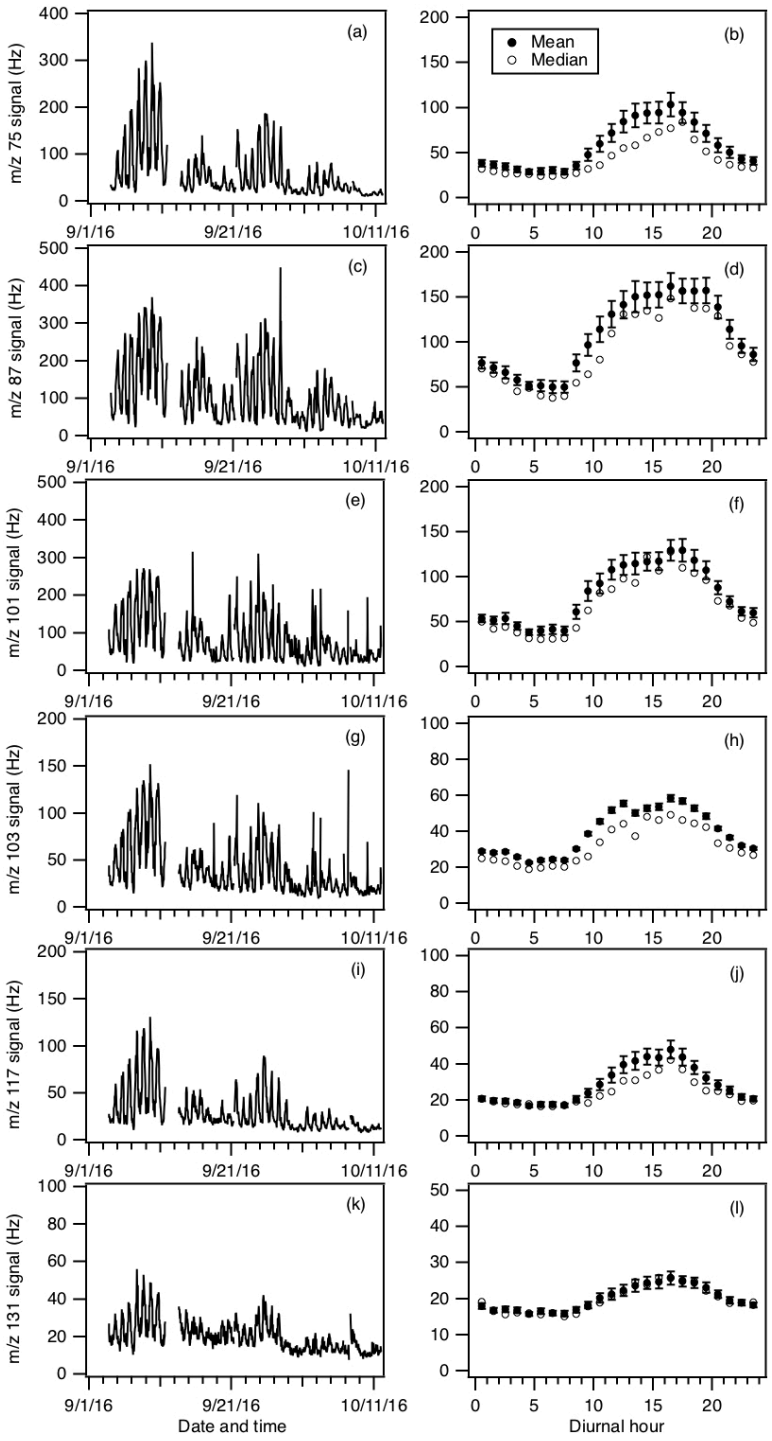

Figure S5: Time series and diurnal profiles of ion signals of organic acids with m/z 75, 87, 101, 103, 117 and 131 measured during the field study. The data are displayed as 1-hour averages. All the signals represent averages in 1-hour intervals and the standard errors are plotted as error bars.

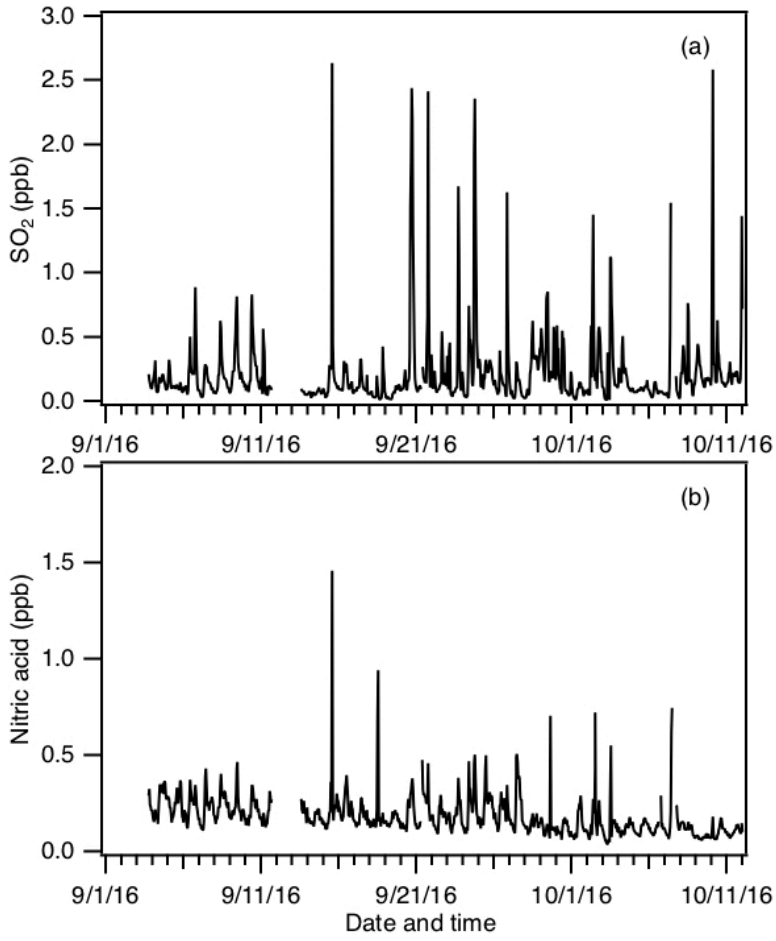

Figure S6: Time series of (a) SO_2 and (b) HNO_3 concentrations measured during the field study. All the data are displayed as 1-hour averages.

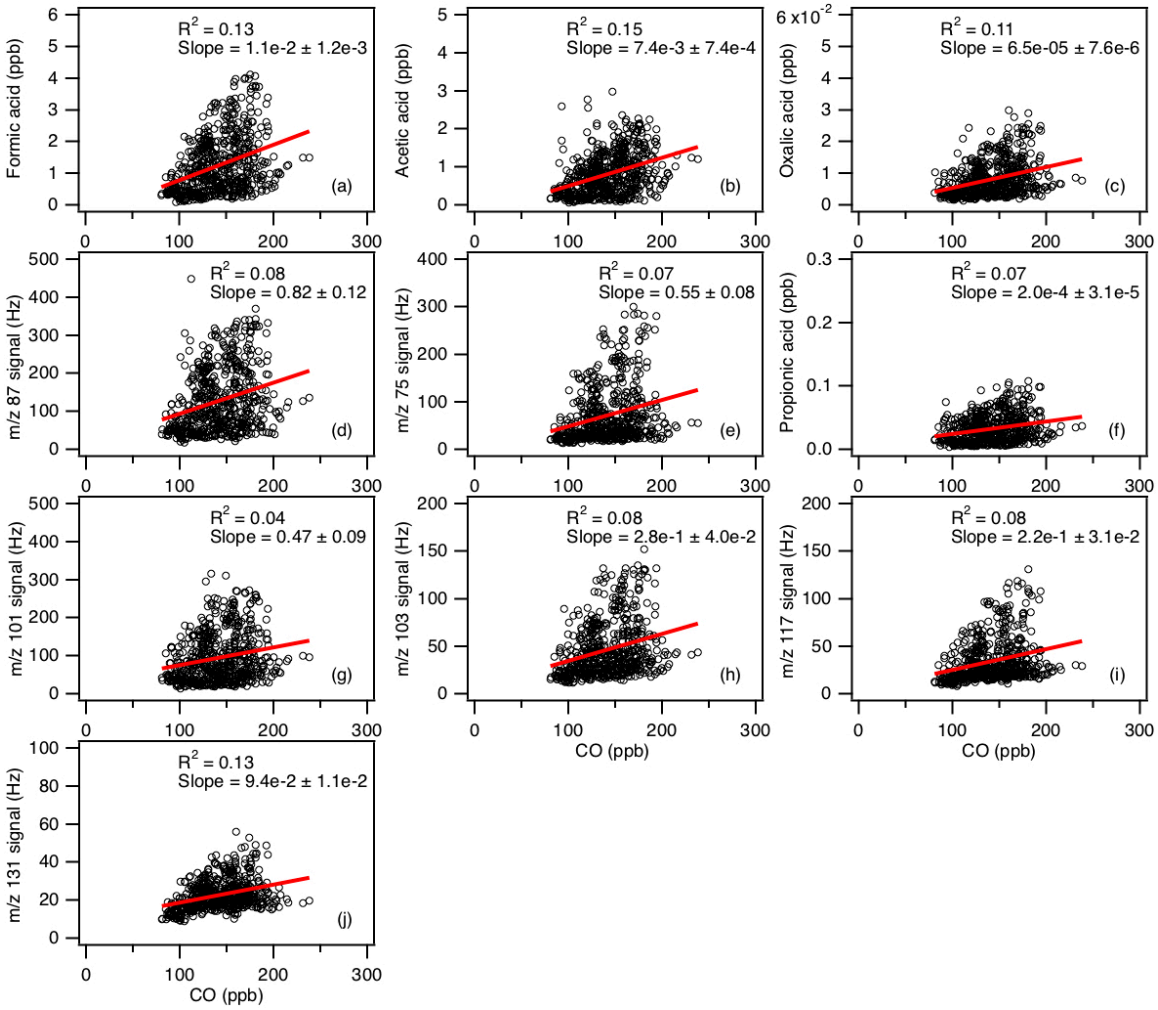

Figure S7: Scatter plots of concentrations (or ion signals) of the measured organic acids with CO concentration. All the data are displayed as 1-hour averages. Red lines shown are linear fits to the data.

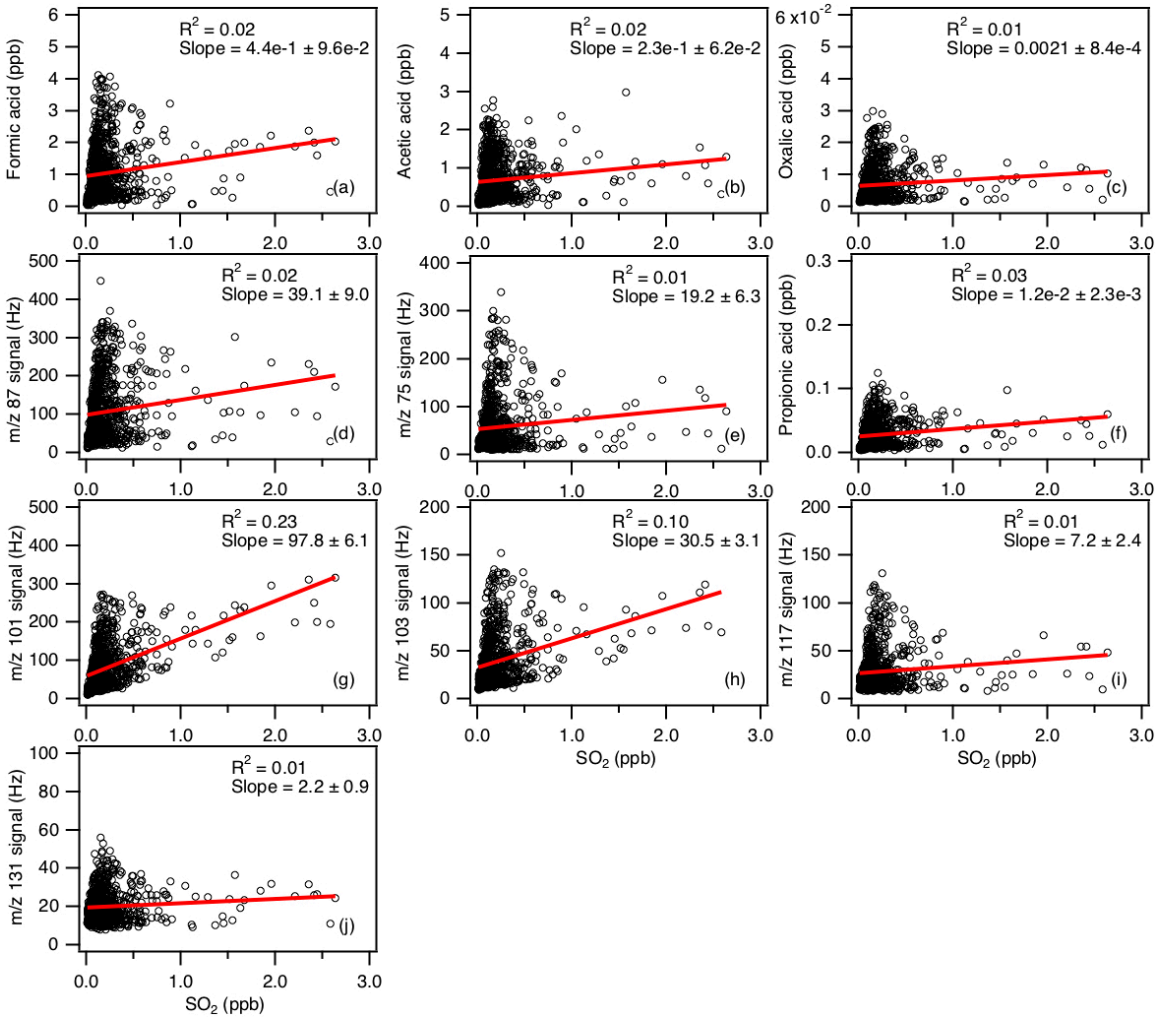

Figure S8: Scatter plots of concentrations (or ion signals) of the measured organic acids with SO_2 concentration. All the data are displayed as 1-hour averages. Red lines shown are linear fits to the data.

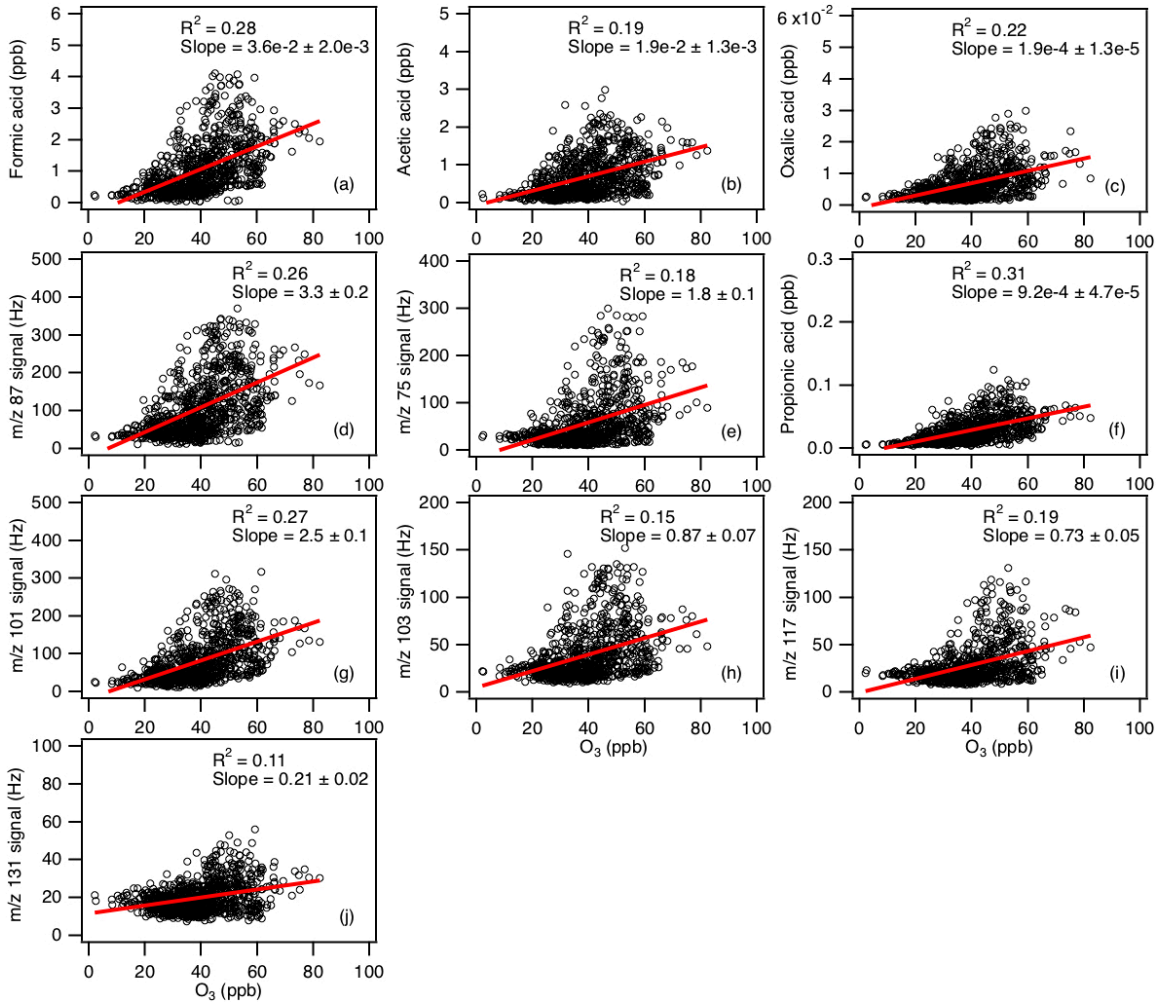

Figure S9: Scatter plots of concentrations (or ion signals) of the measured organic acids with O_3 concentration. All the data are displayed as 1-hour averages. Red lines shown are linear fits to the data.

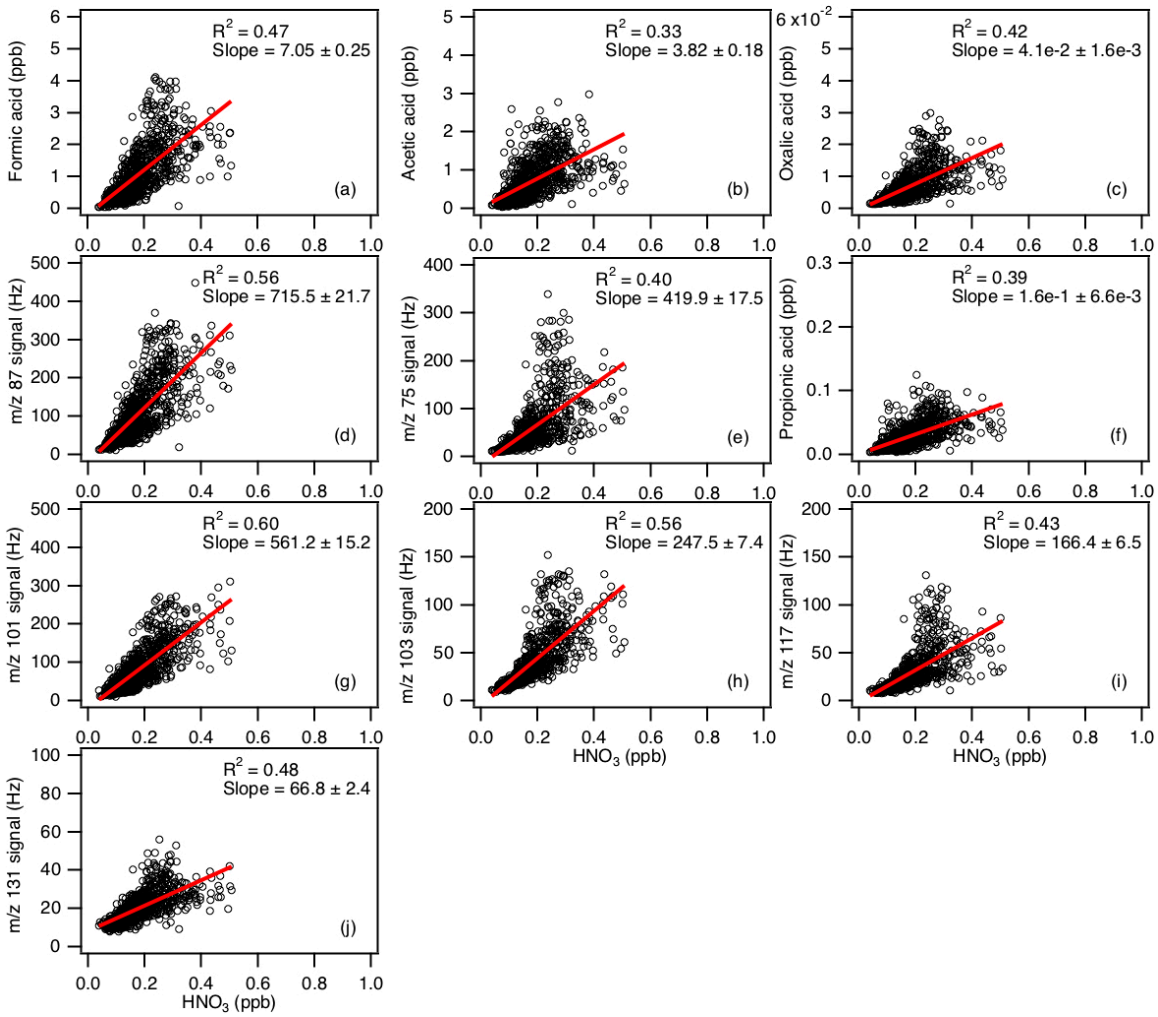

Figure S10: Scatter plots of concentrations (or ion signals) of the measured organic acids with HNO_3 concentration. To exclude periods when the site was affected by urban or power plant emissions, data where HNO_3 > 0.5 ppb are excluded from these scatter plots. All the data are displayed as 1-hour averages. Red lines shown are linear fits to the data.

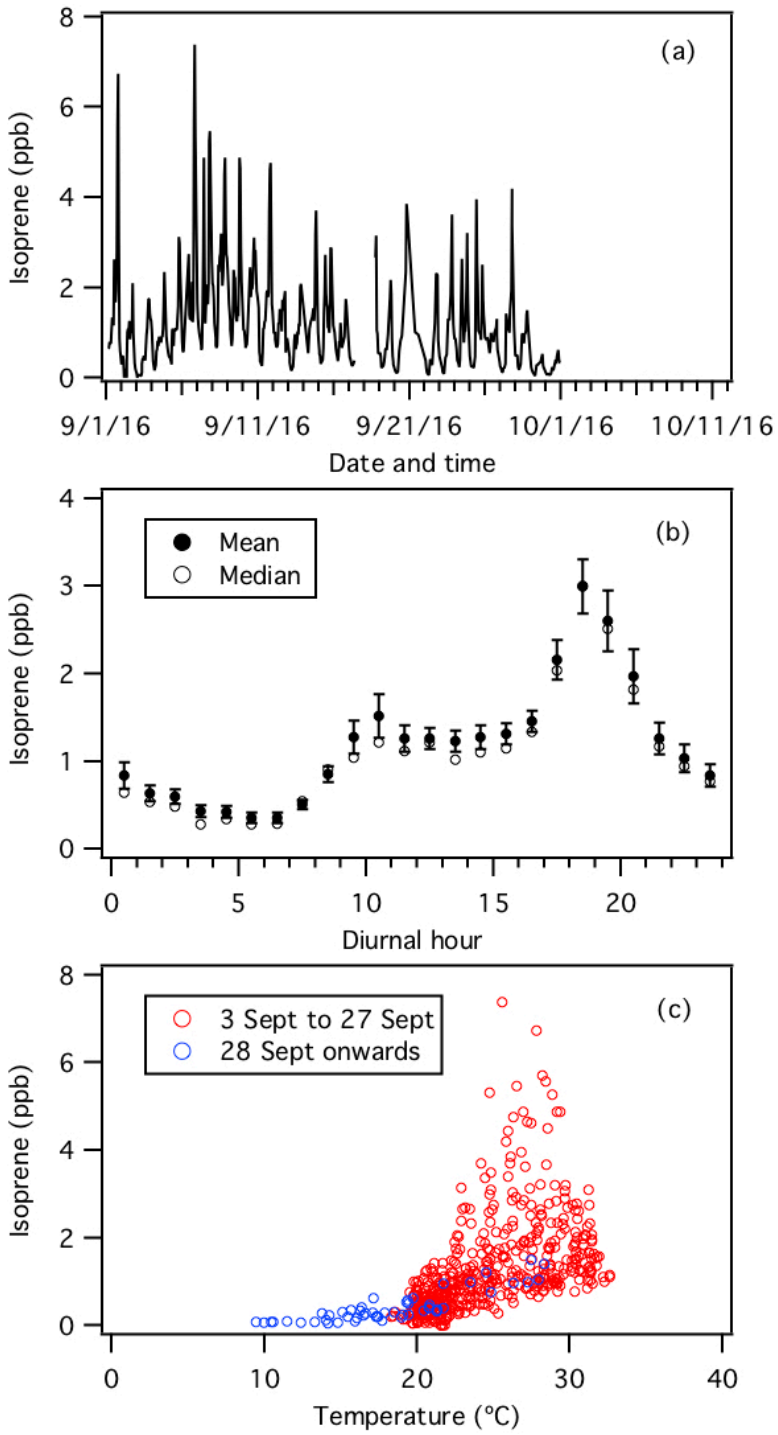

74

75 **Figure S11:** (a) Time series of isoprene concentration during the field study. (b) Diurnal
76 profile of isoprene. All the concentrations represent averages in 1-hour intervals and the
77 standard errors are plotted as error bars. (c) Scatter plot of isoprene concentration with
78 ambient temperature. All the data are displayed as 1-hour averages.

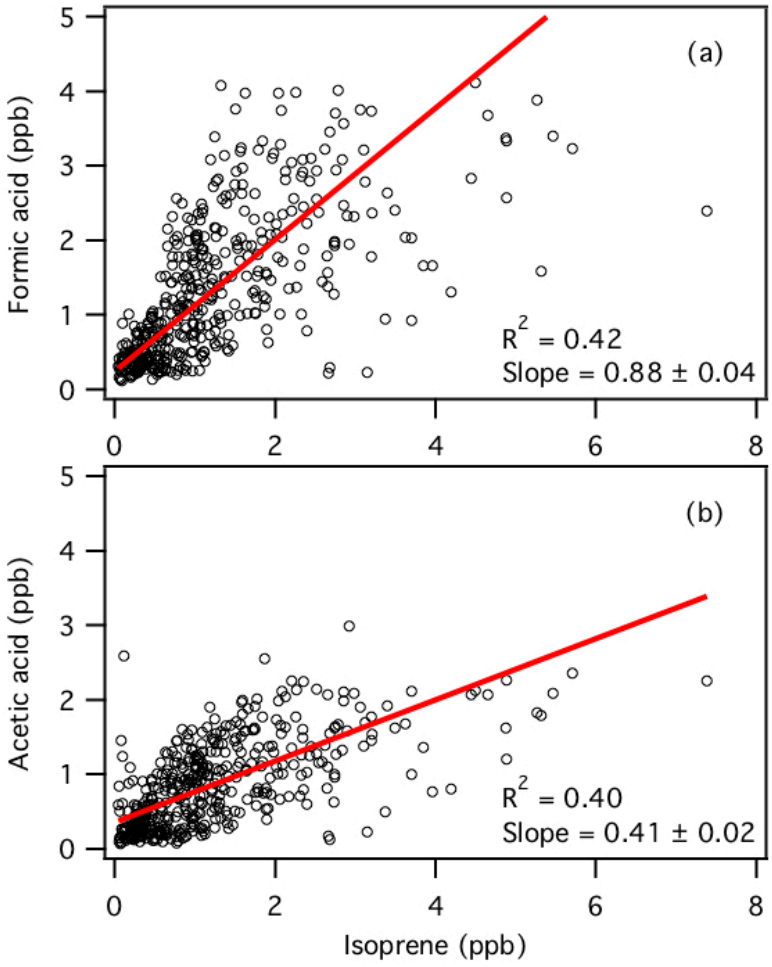

Figure S12: Scatter plots of concentrations of (a) formic and (b) acetic acids with isoprene concentration. All the data are displayed as 1-hour averages. Red lines shown are linear fits to the data.

Table S1a: Comparison of SF_6^- vs. I^- sensitivities of organic acids

Organic Acid	I^- sensitivity ($Hz\ ppt^{-1}$)[a]	SF_6^- sensitivity ($Hz\ ppt^{-1}$)	
		X^-	$X^-•HF$
Formic acid	2.9	1.29 ± 0.22	0.29 ± 0.05
Acetic acid	0.1	1.46 ± 0.29	0.30 ± 0.06
Oxalic acid	0.21	6.38 ± 0.32	0.97 ± 0.05
Butyric acid	Not available	0.41 ± 0.01	0.12 ± 0.004
Glycolic acid	1.1	5.53 ± 0.11	1.64 ± 0.03
Propionic acid	0.066	2.05 ± 0.02	1.26 ± 0.01
Valeric acid	Not available	0.76 ± 0.008	0.35 ± 0.004

[a]The I^- sensitivities shown here are those reported by Lee et al. (2014). The organic acids were detected as cluster ions with iodide ($I(X)^-$).

Table S1b: Comparison of SF_6^- vs. I^- sensitivities of inorganic compounds

Inorganic compound	I^- sensitivity ($Hz\ ppt^{-1}$)[b]	SF_6^- sensitivity ($Hz\ ppt^{-1}$)
SO_2	0.028	2.9
HNO_3	9.0	5.8 for NO_3^-, 0.2 for $NO_3^-•HF$[c]
HCl	0.03	1.4[d]

[b]The I^- sensitivities shown here are those reported by Lee et al. (2018).

[c]The high collision energy used in the CDC promoted the dissociation of $NO_3^-•HF$ ions, causing the low sensitivity at $NO_3^-•HF$.

[d]HCl was detected as SF_5Cl^-.

References

Lee, B. H., Lopez-Hilfiker, F. D., Mohr, C., Kurten, T., Worsnop, D. R., and Thornton, J. A.: An Iodide-Adduct High-Resolution Time-of-Flight Chemical-Ionization Mass Spectrometer: Application to Atmospheric Inorganic and Organic Compounds, Environmental Science & Technology, 48, 6309-6317, 10.1021/es500362a, 2014.

Lee, B. H., Lopez-Hilfiker, F. D., Veres, P. R., McDuffie, E. E., Fibiger, D. L., Sparks, T. L., Ebben, C. J., Green, J. R., Schroder, J. C., Campuzano-Jost, P., Iyer, S., D'Ambro, E. L., Schobesberger, S., Brown, S. S., Wooldridge, P. J., Cohen, R. C., Fiddler, M. N., Bililign, S., Jimenez, J. L., Kurtén, T., Weinheimer, A. J., Jaegle, L., and Thornton, J. A.: Flight Deployment of a High-Resolution Time-of-Flight Chemical Ionization Mass Spectrometer: Observations of Reactive Halogen and Nitrogen Oxide Species, Journal of Geophysical Research: Atmospheres, 0, doi:10.1029/2017JD028082, 2018.